# Protection against lead–free solder in wave–soldering by Ti/TiC coatings prepared by filtered cathodic arc deposition

**Article** *in* Surface and Coatings Technology · June 2016

Impact Factor: 2 · DOI: 10.1016/j.surfcoat.2016.06.008



**8 authors**, including:

Zhongzhen Wu

Peking University

**24** PUBLICATIONS **61** CITATIONS

SEE PROFILE

Feng Pan

Peking University

**87** PUBLICATIONS **1,090** CITATIONS

SEE PROFILE

Surface & Coatings Technology xxx (2016) xxx-xxx

Contents lists available at ScienceDirect

Surface & Coatings Technology

journal homepage: www.elsevier.com

# Protection against lead-free solder in wave-soldering by Ti/TiC coatings prepared by filtered cathodic arc deposition

Shu Xiao,[a, c] Zhongzhen Wu,[a, *] Liangliang Liu,[a] Ricky K.Y. Fu,[c, *] Wan Li,[c] Xiubo Tian,[b] Paul K. Chu,[c] Feng Pan [a]

[a] School of Advanced Materials, Peking University Shenzhen Graduate School, Shenzhen 518055, China
[b] State Key Laboratory of Advanced Welding and Joining, Harbin Institute of Technology, Harbin 150001, China
[c] Department of Physics and Materials Science, City University of Hong Kong, Tat Chee Avenue, Kowloon, Hong Kong, China

ARTICLE INFO

*Article history:*
Received 23 March 2016
Received in revised form 19 May 2016
Accepted 3 June 2016
Available online xxx

*Keywords:*
Ti/TiC
Wave soldering holder
FCVA
Tin-repellent

ABSTRACT

Lead-free solder is increasingly used in the wave soldering but corrosion of the stainless steel holders frequently occurs and produces deleterious effects. To enhance the service life, a Ti/TiC coating is deposited by filtered cathodic vacuum arc (FCVA) on the stainless steel holders. The morphology, structure, composition, microhardness, wear resistance, electron chemical corrosion, and wetting properties against solder are investigated. The results show that not only good frictional properties and corrosion resistance are achieved by the Ti/TiC coatings, but also good tin repelling and hydrophobic characteristics are observed. The Ti/TiC coating provides excellent protection against corrosion of lead-free solder in wave soldering.



## 1. Introduction

According to the Waste Electrical and Electronic Equipment (WEEE) and Restriction of Certain Hazardous Substances (RCHS) regulations proposed in 2003, lead has been forbidden in electronic products since 2006 and lead-free solder has been used to replace the traditional Sn-Pb solder [1–3]. However, the larger Sn content in lead-free solder leads to a higher welding temperature [4] consequently increasing the risk of corrosion of stainless steel components in wave soldering equipment [5–7] such as the solder container, wave wheel rotor, and duckbilled holder. Residual solder adhering to the soldering holders also requires mechanical removal as shown in Fig. 1.

There are two approaches to mitigate the problems by replacing the stainless steel with other materials and conducting surface modification. For example, Ti and Ti-alloys and cast iron have been used to instead of stainless steel to produce the holders and they exhibit better tin repellence, suggesting the effective roles of Ti and C [8]. However, Ti and Ti-alloys are quite expensive and pollution of Ti limits the service life. Cast iron possesses poor formability boding well for components with a complex shape and surface modification of the holders has become increasingly popular. Hu, et al. [9] studied the corrosion resistance of the SS holders after N ions implantations and obtained similar results as Ti alloys. Morris, et al. [8] studied the corrosion resistance of Ti, cast iron, nitride and $Cr_xC_y$ coatings in the liquid lead-free solder and observed the key role of C in the coatings in tin repellence. Additionally, PPS and nylon 66 coatings were prepared on holding strips and components made of stainless steel to hinder adhesion and corrosion and the modified holders were found to have small surface energy against tin solders thereby inducing wetting resistance [10,11]. Nevertheless, organic coatings tend to have poor mechanical performance and also degrade quickly during prolonged use at a high soldering temperature. In this work, Ti/TiC coatings are prepared on stainless steel holders to provide protection. The mechanical properties, wetting characteristics, and corrosion resistances against tin solders were investigated.

## 2. Experimental details

The experiments were performed in vacuum chamber with a diameter of 100 cm and height of 80 cm. After the chamber was evacuated to a base pressure of $3 \times 10^{-3}$ Pa, the carrier gas (Ar, 99.999% pure) and reactive gas ($C_2H_2$, 99.8% pure) were introduced through a leak valve. A Ti target (50 mm in diameter, 40 mm thick, and 99.9% pure) was mounted in the cathodic vapor arc source. To balance the deposition rate and the amount of "macro-particles", a straight magnetic filter was assembled between the cathodic arc and the vacuum. Silicon (100) and stainless steel holders were used as substrates. Prior to loading into the chamber, the substrates were ultrasonically cleaned in ethanol and acetone for 20 min at room temperature. The substrates were placed at a distance of 10 cm from the exit of the magnetic filter and no external heating was applied during the process. The experiments were carried out in four stages. Firstly, plasma etching was performed with Ar at 1 kV. Secondly, a Ti layer was deposited on the samples by FCVA with the current of 60 A and the voltage of 43 V in argon to increase the adhesion between the film and substrate. Thirdly, the TiC film was deposited by reactive FCVA with the current of 60 A and the voltage of 43 V using the two gases at different

* Corresponding authors.
Email addresses: wuzz@pkusz.edu.cn (Z. Wu); rickyfu@plasmatechnol.com (R.K.Y. Fu)

http://dx.doi.org/10.1016/j.surfcoat.2016.06.008
0257-8972/

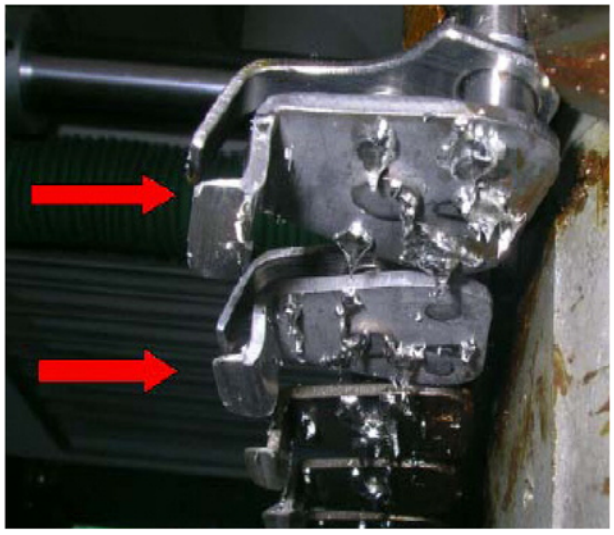

**Fig. 1.** Lead-free solder on the wave soldering holders.

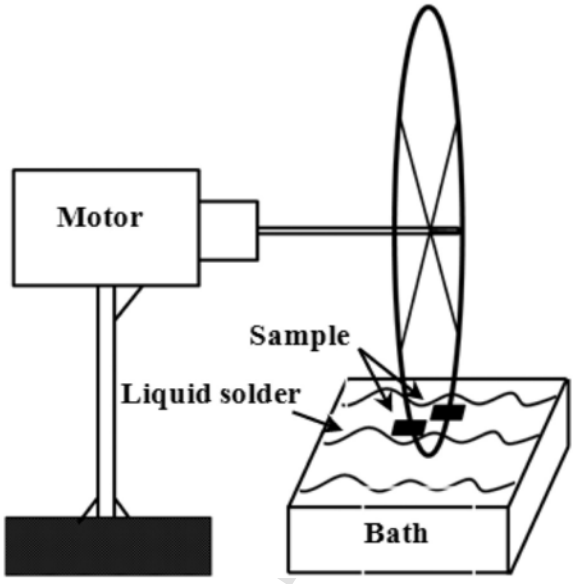


**Fig. 2.** Schematic diagram of the tin-repellent property test.

$C_2H_2$ partial pressure from 0.1 Pa to 0.7 Pa and different bias from 50 V to 200 V. Finally, the samples were cooled naturally in vacuum.

The structure was determined by X-ray diffraction (Bruker D8 Advance) in the continuous scanning mode using Cu Kα radiation (λ = 0.15418 nm) at room temperature. The test angle range (2θ) is from 10° to 80° and the step size is 0.1°. The surface morphology was examined by field-emission scanning electron microscopy (FESEM, ZEISS SUPRA® 55). The HVS-1000 micro-hardness tester was used to determine the micro-hardness of the coatings with a load of 10 g for 20 s. The data were averaged by 10 micro-hardness measurements. The wear resistance was evaluated by a ball-on-disk tester under ambient conditions (relative humidity was 25 ± 1 RH% and temperature of 20 ± 1 °C). Sliding was performed against a Φ6.636 mm SiC ball with a 100 N load at a speed of 80 rpm with a wear radius of 3 mm. The electro-chemical corrosion test was performed on a Reference 600 Electrochemical Analyzer. The reference electrode was the saturated KCl solution and the auxiliary electrode was platinum. The solution was 3.0 wt% NaCl solution and polarization was performed at a scanning rate of 3 mV/s.

The tin-repellent property was assessed by simulating the practice wave soldering process by a homemade device shown in Fig. 2. The samples were dipped into the liquid tin solder at 280 °C and then pulled-out after 5 s similar to the practice in commercial wave soldering. After repeating the process for 100 times, the sample was observed by optical microscopy and the mass difference was determined on a precision electronic balance (0.001 g). The surface tension in liquid solder was tested on a wetting balance meter at 280 °C with the speed, depth, and duration being 5 mm/s, 3 mm and 20 s, respectively. An optical contact angle instrument (Dataphysics, Inc.) was used to observe the solder droplet (5 g solder) after the heating-cooling cycle. The solder melted and formed a droplet which rolled freely on the coating at 280 °C and higher. As the temperature drooped, the spherical droplet remained on the coating.

## 3. Results and discussion

### *3.1. Structure and morphology*

The XRD patterns of the Ti/TiC coatings deposited on the stainless steel samples by FCVA at different $C_2H_2$ partial pressure are depicted in Fig. 3. Except the peaks of the substrate, only Ti and TiC peaks can be observed. Ti peaks which may be attributed by the transition layer and the unreacted Ti show Ti (100), Ti (101) and Ti (103) preferred orientations with the 2θ of 35.04°, 36.57°, 40.10°, respectively. When the $C_2H_2$ partial pressure is 0.1 Pa, Ti is dominant in the coating. Although the TiC diffraction peaks are not obvious, TiC (111), TiC (200), and TiC (220) located at 36.57°, 41.86° and 59.65°, respectively can be recognized from the XRD spectrum of the Ti/TiC coatings and the preferential orientation is TiC (111) which possesses a low free energy. When the $C_2H_2$ partial pressure is raised from 0.1 to 0.7 Pa, the Ti peaks decrease but the TiC ones increase quickly, indicating a gradual increase of the dominant phase of face-center-cubic TiC [12,13]. However, the preferential orientation of TiC becomes TiC (200), suggesting a low surface energy at the high $C_2H_2$ partial pressure [14–16].

The surface morphology SEM images of the Ti/TiC coatings prepared at different $C_2H_2$ partial pressure are presented in Fig. 4. Only

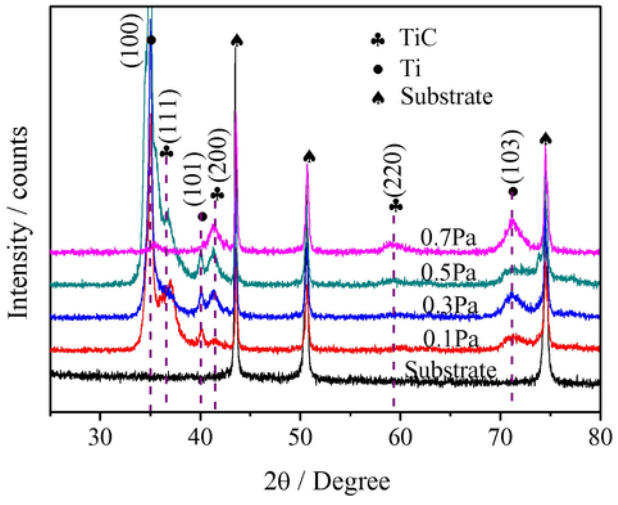


**Fig. 3.** XRD patterns of the Ti/TiC coatings deposited at different $C_2H_2$ partial pressure.

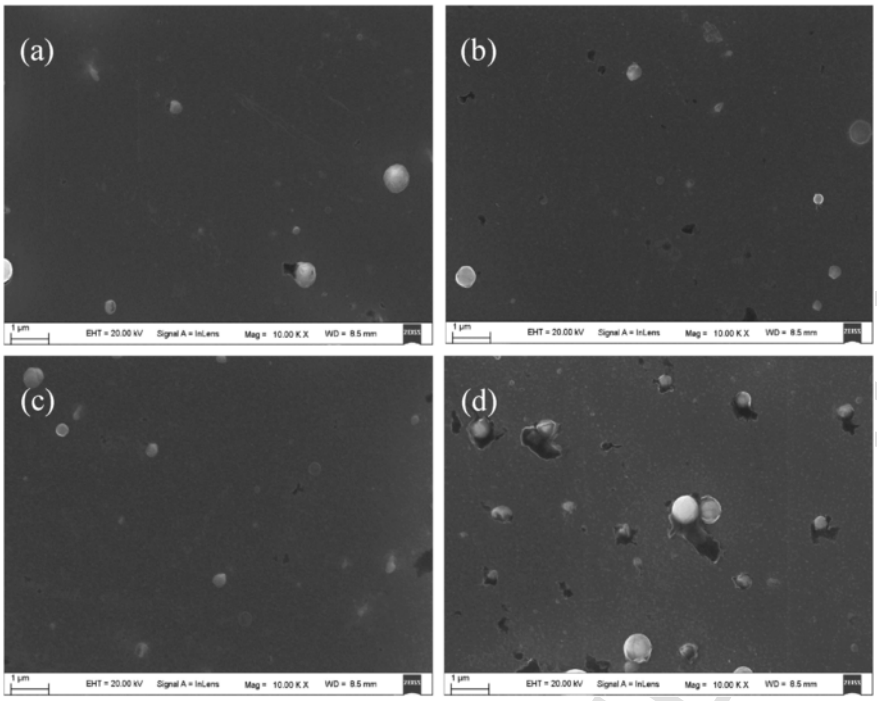


**Fig. 4.** Surface morphology SEM images of the Ti/TiC coatings deposited on silicon at $C_2H_2$ partial pressure of (a) 0.1 Pa, (b) 0.3 Pa, (c) 0.5 Pa, and (d) 0.7 Pa.

a few macro-particles can be observed on the surface of the coatings compared to those prepared by conventional cathodic arc deposition without filtering [17,18]. When the $C_2H_2$ partial pressure is small, the surface of the coating is smooth and dense. However, much macro-particles and defects produce on the surface with increasing the $C_2H_2$ partial pressure to 0.7 Pa. The cross-sectional SEM images of the Ti/TiC coatings are presented in Fig. 5. A 200 nm thick Ti interface layer and a 1 μm thick TiC layer can be identified. The Ti interface layer is crucial to good adhesion between the TiC coating and substrate [19–21]. A typical columnar and dense structure is observed from the TiC coatings prepared at $C_2H_2$ partial pressure of 0.1 Pa, 0.3 Pa, and 0.5 Pa as shown in Fig. 5a, b, c, respectively, whereas the coating deposited at 0.7 Pa shows a cluster structure (Fig. 5d) due to the large amount of $C_2H_2$ [16,22,23].

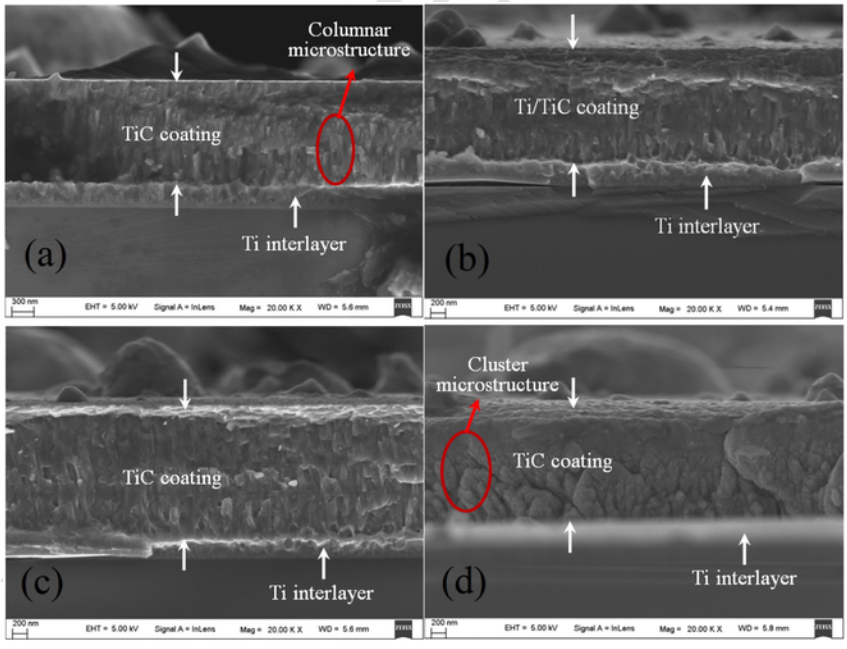


**Fig. 5.** Cross-sectional SEM images of the Ti/TiC coatings deposited on silicon at $C_2H_2$ partial pressure of (a) 0.1 Pa, (b) 0.3 Pa, (c) 0.5 Pa, and (d) 0.7 Pa.

### 3.2. Microhardness

The microhardness of the Ti/TiC coatings is observed in Fig. 6. Owing to the thickness of the coatings (1 μm) which are smaller than 5 times of the indentation depth (between 276.3 nm and 312.7 nm), the hardness includes contributions from the substrate making them smaller than the actual value [19,24]. All the coatings are harder than the substrate and with increasing $C_2H_2$ partial pressures, the microhardness increases initially and begins to decrease when the $C_2H_2$ partial pressure is 0.5 Pa (Fig. 6a). The highest microhardness is 1247 HV corresponding to stoichiometric TiC according to XRD. Excessive $C_2H_2$ produces an amorphous carbon-rich phase in the coating and consequently, the microhardness decreases [25]. The microhardness dependence on the bias is illustrated in Fig. 6b. The microhardness of the Ti/TiC coatings increases monotonically with increasing bias and the highest value (1335 HV) is achieved at − 200 V. Generally, both ion bombardment and sputtering of the loose deposition and defects occur to improve the density, crystallinity, and microhardness of the coatings [26].

### 3.3. Tribological properties

The tribological behavior of the Ti/TiC coatings prepared at different $C_2H_2$ partial pressure and bias is shown in Fig. 7. An obvious decrease in the friction coefficient is observed from the coatings compared to the stainless steel substrate. The smallest friction coefficient of 0.11 is achieved when the $C_2H_2$ partial pressure is between 0.3 and 0.5 Pa at the bias of − 100 V. As the $C_2H_2$ partial pressure is increased from 0.1 Pa to 0.5 Pa, the friction coefficients decrease from 0.33 to 0.10 because of the large C contents in the coatings. If the $C_2H_2$ partial pressure is further increased, more defects are formed (confirmed by SEM) affecting the friction coefficient as shown in Fig. 7a. When different biases are used, the friction coefficients are similar although the optimal bias is − 100 V. The bias produces two main effects. Firstly, more Ti ions are attracted to the samples [26], at a high bias and the Ti content in the coating goes up. Secondly, the defects in the coatings decrease giving rise to a large coating density [19,27]. Therefore, the smaller friction coefficient at a low bias may be attributed to the improved coating density and mechanical properties and the large friction coefficient at a high bias stems from the large Ti concentration rendering the coating non-stoichoimetric.

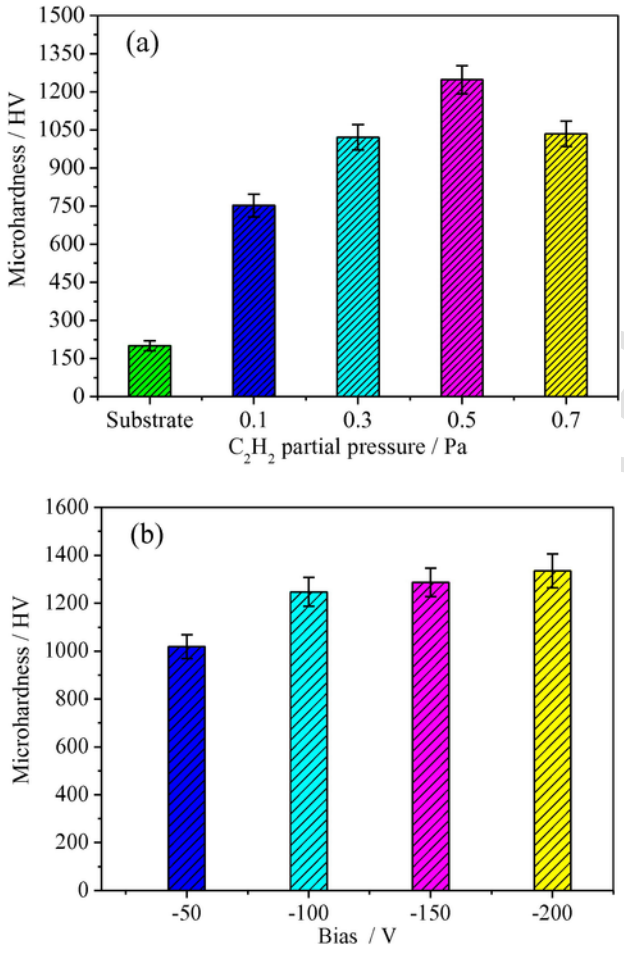


**Fig. 6.** Micro-hardness of the Ti/TiC coatings produced at: (a) different $C_2H_2$ partial pressure and (b) different bias.

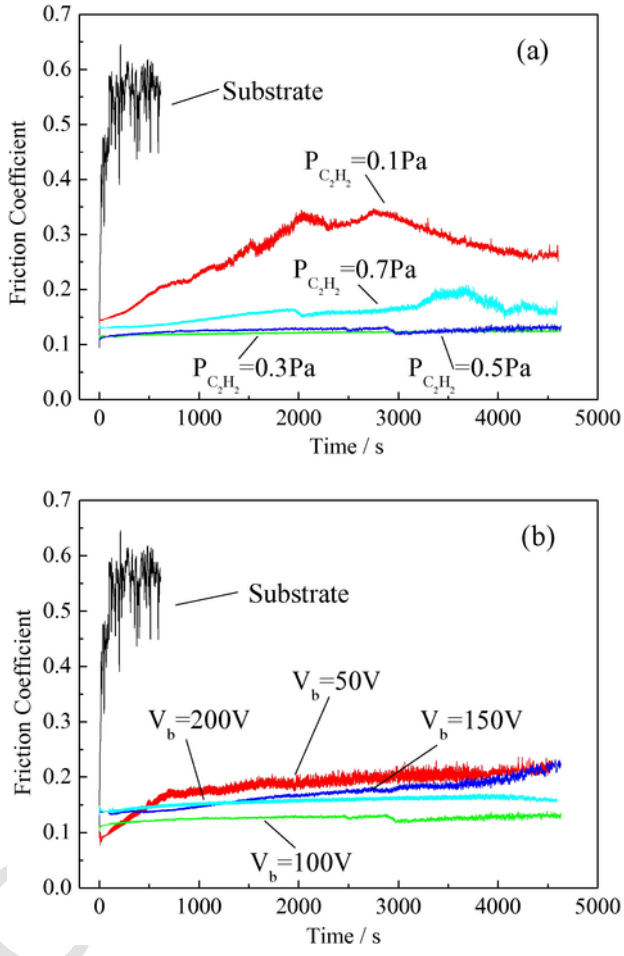


**Fig. 7.** Friction coefficients of the Ti/TiC coatings prepared at (a) different $C_2H_2$ partial pressure and (b) different bias.

### 3.4. Corrosion resistance

The polarization curves of the Ti/TiC coatings prepared at different $C_2H_2$ partial pressure and bias are displayed in Fig. 8. The coated samples exhibit larger corrosion potentials and smaller corrosion currents than the substrates indicating better corrosion resistance. When the $C_2H_2$ partial pressure is 0.5 Pa, the best corrosion resistance with

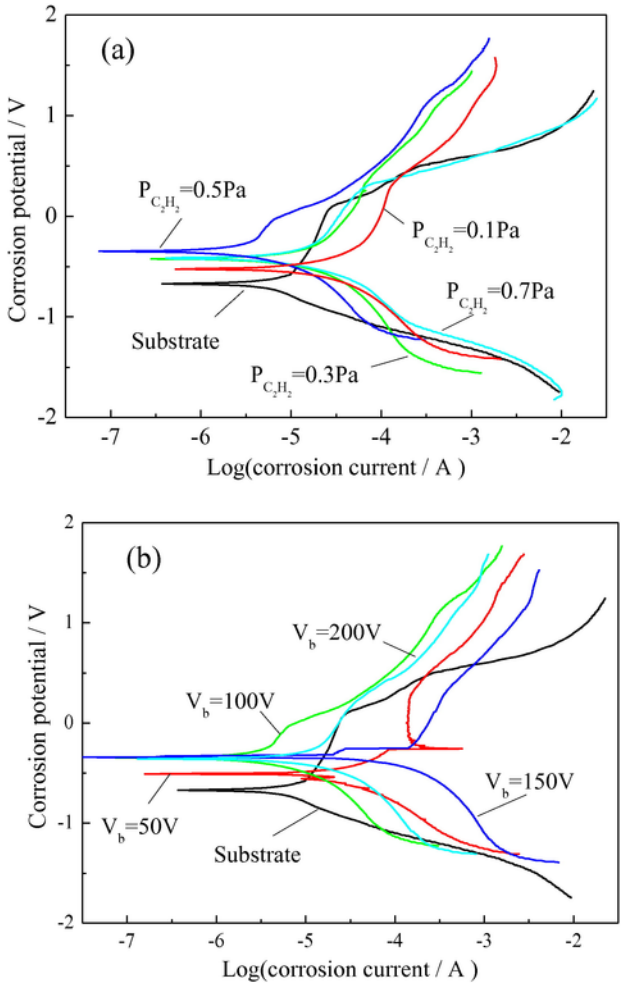


**Fig. 8.** Polarization curves of the Ti/TiC coatings prepared at (a) different $C_2H_2$ partial pressure and (b) different bias.

the corrosion potentials increasing from − 0.671 V to − 0.288 V and the corrosion currents decreasing from 51 μA to 1.84 μA (Fig. 8a) are observed. The stoichiometric C/Ti ratio is 0.97, which yields the best mechanical properties as described before. The corrosion resistance of the coatings decreases slightly if the $C_2H_2$ partial pressure is too high as the increase of corrosion tunnels throughout the coating. Fig. 8b illustrates the effects of the bias to the corrosion resistance. As the bias is increased, obvious improvement is observed because the large density reduces the corrosion tunnels in the coating and prevents further corrosion. However, when the bias is larger than 100 V, no significant enhancement in the corrosion resistance is observed suggesting that it is the optimal value.

### *3.5. Tin-repellence*

The contact angles on the Ti/TiC coatings for liquid lead-free solder in comparison with Ti and cast iron using the modified sessile drop method are shown in Fig. 9. All the samples exhibit a non-wetting behavior with the average contact angles on Ti, cast iron, and TiC coating being 131.35°, 133.9°, and 133.95°, respectively. Compare to Ti and cast iron, the Ti/TiC coating has better hydrophobicity probably due to the synergistic effects of Ti and C [28].

In order to assess the durability and lifetime of the coated samples, Fig. 10 shows the surface images of stainless steel, Ti, cast iron and Ti/TiC coating after immersion in the liquid solder 100 times. In the beginning of immersion, there is no visible adhesion on any sample. However, corrosive pits can be observed from the stainless steel sample after immersion and eventually, large pieces of solder stick to the sample surface and must be removed mechanically similar to the phenomenon shown in Fig. 1. In comparison, a few small solder droplets adhere to the other three samples. To quantitative determine the effects, the weight of the solder adhered on the sample after immersion for 100 times is determined and the results are shown in Fig. 11. The weight of the solder on Ti, cast iron and Ti/TiC coatings is about two orders of magnitude less than that on the stainless steel substrate. The best tin-repelling efficiency is again observed from the Ti/TiC coating which shows the least weight of 0.001 g. The improvement can be explained by the small surface energy of the coatings [27] and the similar hydrophobic property to liquid solder.

## 4. Conclusions

Ti/TiC coating are deposited on stainless steel holders by FCVA to improve the corrosion resistance and repellent performance against liquid tin solder. The structures, morphology, mechanical properties of the Ti/TiC coatings depend on the $C_2H_2$ partial pressure and bias. The optimal $C_2H_2$ partial pressure and bias are 0.5 Pa and − 100 V, respectively. The microhardness of the optimal Ti/TiC coating is 1335 HV which is 7 times larger than that of the stainless steel substrate. The TiC coatings also have smaller friction coefficients and better corrosion resistance. Compared to Ti and cast iron, the TiC coatings show larger contact angles and have better repellent properties against liquid solder. Hence, the Ti/TiC coatings improve the protection of the stainless steel holders and have potential in wave soldering involving lead-free solder.

## Acknowledgements

This work was financially supported jointly by Natural Science Foundation of China (No. 51301004, U1330110), Shenzhen Science and Technology Research Grant (JCYJ20140903102215536 and JCYJ20150828093127698), and City University of Hong Kong Applied Research Grant (ARG) No. 9667104.

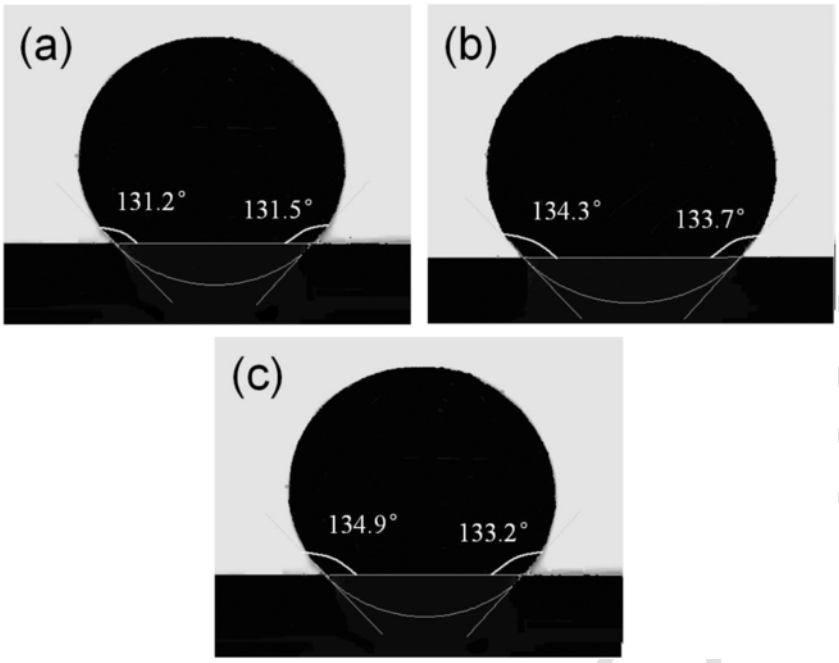


**Fig. 9.** Contact angles for the lead-free solder on (a) Ti, (b) cast iron, and (c) Ti/TiC.

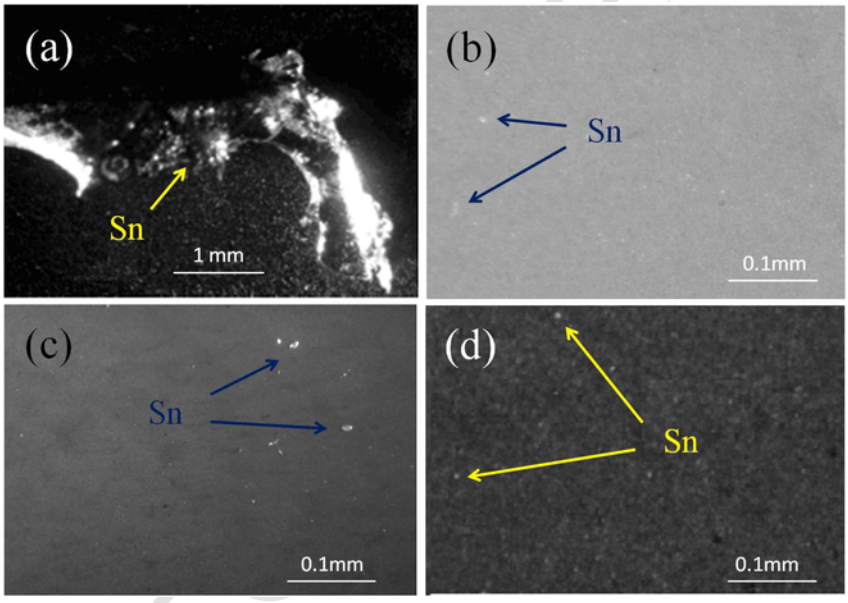


**Fig. 10.** Micrographs showing the degree of tin solder adhesion on the different samples: (a) stainless steel, (b) Ti, (c) cast iron, and (d) Ti/TiC.

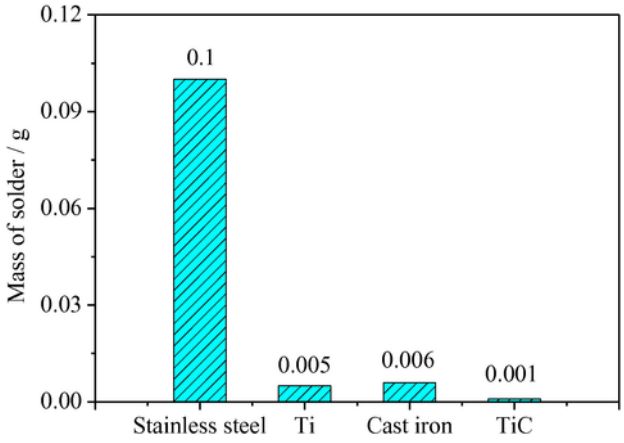


**Fig. 11.** Weight of lead-free solder on the different samples: (a) stainless steel, (b) Ti, (c) cast iron, and (d) Ti/TiC.

## References


[1] A.A. El-Daly, H. El-Hosainy, T.A. Elmosalami, W.M. Desoky, J. Alloys Compd. 653 (2015) 402.
[2] S. Liu, S.B. Xue, J. Mater. Sci. Mater. Electron. 26 (2015) 9424.
[3] G. Chen, F. Wu, C. Liu, V.V. Silberschmidt, Y.C. Chan, J. Alloys Compd. 656 (2016) 500.
[4] K. Zeng, K.N. Tu, Mater. Sci. Eng. R 38 (2002) 55.
[5] A. Forsten, H. Steen, I. Wiling, Surf. Mt. Technol. 12 (2000) 29.
[6] T. Takemoto, M. Takemoto, Surf. Mt. Technol. 18 (2006) 24.
[7] T. Takemoto, M. Takemoto, ECODIM-EcoDesign, 10, 2005908.
[8] M. Jim, J. Matthew, APEX, 2003.
[9] Q. Hu, A.G. Huang, Z.S. Li, Eqpt. For Electron. Products MFG, 1, 200553.
[10] L.M. Pan, Hangzhou Electron. Technol. 2 (1991) 32.
[11] Z.L. Liu, Y.H. Guo, D.H. Chen, Eng. Plastics Appl. 41 (2003) 19.
[12] Y. Diao, K. Zhang, Appl. Surf. Sci. 352 (2015) 163.
[13] D.R. McKenzie, Y. Yin, W.D. McFall, Condens. Matter 8 (1996) 5883.
[14] U.C. Oh, J. Appl. Phys. 74 (1993) 1692.
[15] J. Pelleg, L.Z. Zevin, S. Lungo, Thin Solid Films 197 (1991) 117.
[16] A.A. Voevodin, M.A. Capano, S.J.P. Laube, M.S. Donley, J.S. Zabinski, Thin Solid Films 298 (1997) 107.
[17] X. Zhang, H. Liang, Z. Wu, X. Wu, H. Zhang, Nucl. Inst. Methods Phys. Res. B 307 (2013) 115.
[18] Z. Xu, H. Sun, Y.X. Leng, X. Li, W. Yang, N. Huang, Appl. Surf. Sci. 328 (2015) 319.
[19] F. Bülbül, İ. Efeoğlu, Met. Mater. Int. 16 (2010) 573.
[20] J. Li, Y. Yang, G. Feng, X. Luo, Q. Sun, N. Jin, Appl. Surf. Sci. 286 (2013) 240.
[21] H.A. Chaliyawala, G. Gupta, P. Kumar, G. Srinivas, Siju, H.C. Barshilia, Surf. Coat. Technol. 276 (2015) 431.
[22] Y.R. Xu, H.D. Liu, Y.M. Chen, M.I. Yousaf, C. Luo, Q. Wan, Appl. Surf. Sci. 349 (2015) 93.
[23] M. Samuelsson, K. Sarakinos, H. Högberg, E. Lewin, U. Jansson, B. Wälivaara, Surf. Coat. Technol. 206 (2012) 2396.
[24] U.H. Hwang, Thin Solid Films 254 (1995) 16.
[25] M.J. Mosayebi, S.R. Hosseini, Surf. Eng. 31 (2015) 96.
[26] X. Liu, X. Lv, H. Dong, C. Li, C. Bai, Metall. Mater. Trans. A 46 (2015) 4783.
[27] Q. Lin, P. Shen, L. Yang, S. Jin, Q. Jiang, Acta Mater. 59 (2011) 1898.
[28] C.K. Leong, F. Emmanuelle, Mater. Sci. Eng. A 278 (2000) 162.